land

MDPI

Article

Integrating Erosion Potential Model (EPM) and PAP/RAC Guidelines for Water Erosion Mapping and Detection of Vulnerable Areas in the Toudgha River Watershed of the Central High Atlas, Morocco

Kamal Elbadaoui [1], Soukaina Mansour [2], Mustapha Ikirri [3], Kamal Abdelrahman [4], Tamer Abu-Alam [5,6,*] and Mohamed Abioui [3,7,*]

1 Department of Geology, Faculty of Sciences Semlalia, Cadi Ayad University, Marrakech 40000, Morocco
2 Department of Earth and Environmental Sciences, Faculty of Sciences and Technique of Al Hoceima, Abdelmalek Essaadi University, Al Hoceima 32003, Morocco
3 Department of Earth Sciences, Faculty of Sciences, Ibnou Zohr University, Agadir 80000, Morocco
4 Department of Geology & Geophysics, College of Science, King Saud University, Riyadh 11451, Saudi Arabia
5 The Faculty of Biosciences, Fisheries and Economics, UiT The Arctic University of Norway, 9037 Tromsø, Norway
6 OSEAN—Outermost Regions Sustainable Ecosystem for Entrepreneurship and Innovation, University of Madeira, Colégio dos Jesuítas, 9000-039 Funchal, Portugal
7 MARE-Marine and Environmental Sciences Centre—Sedimentary Geology Group, Department of Earth Sciences, Faculty of Sciences and Technology, University of Coimbra, 3030-790 Coimbra, Portugal
* Correspondence: tamer.abu-alam@uit.no (T.A.-A.); m.abioui@uiz.ac.ma (M.A.)

check for updates

Citation: Elbadaoui, K.; Mansour, S.; Ikirri, M.; Abdelrahman, K.; Abu-Alam, T.; Abioui, M. Integrating Erosion Potential Model (EPM) and PAP/RAC Guidelines for Water Erosion Mapping and Detection of Vulnerable Areas in the Toudgha River Watershed of the Central High Atlas, Morocco. *Land* **2023**, *12*, 837. https://doi.org/10.3390/land12040837

Academic Editors: Giandomenico Foti, Giuseppe Barbaro, Giuseppe Bombino and Daniela D'Agostino

Received: 11 February 2023
Revised: 1 April 2023
Accepted: 3 April 2023
Published: 6 April 2023

Abstract: This study aimed to evaluate the extent and severity of water erosion in the Toudgha river catchment in the Central High Atlas of Morocco using two different erosion models, the Erosion Potential Model (EPM) and the Priority Actions Programme/Regional Activity Centre (PAP/RAC) model. From the modeling results, the catchment was affected by varying degrees of erosion, ranging from "very slight" to "excessive", with different locations identified under each model. The very high erosion areas were located in the extreme northwest of the catchment area for both of the applied models, covering 9.65% (according to PAP/RAC) and 8.56% (EPM) of the total area primarily driven by factors such as intense rainfall events, limited vegetation cover, high soil erodibility due to low organic matter content and coarser soil texture, and human activities such as overgrazing and land use changes, which exacerbate the effects of these natural factors on water erosion in these semi-arid areas. The study's findings suggest that erosion is a significant concern in these environmental areas and provide valuable information for designing effective erosion control measures and guiding soil and environmental management practices. Both models effectively simulated the erosion phenomenon and provided useful tools for soil and environmental management. The EPM model can be used to design effective erosion control measures, while the PAP/RAC model can be used to develop a comprehensive strategy for the sustainable management of the catchment area. These results have implications for the implementation of effective erosion control measures in mountainous watersheds and highlight the need for further research in this area.

Keywords: erosion potential model (EPM); PAP/RAC model; water erosion; risk; Toudgha river catchment; Morocco

1. Introduction

In recent years, various methods for assessing and estimating erosion intensity and sediment production have been developed. To improve model performance, sensitivity analyses are increasingly being used to reduce errors that arise from the model's concept. Soil erosion caused by surface water is a significant global problem that is both a major land

degradation issue and a critical environmental hazard [1–3]. Human development and inappropriate land use have intensified soil erosion in many parts of the world [4,5]. Water erosion is responsible for the production of millions of tons of sediment worldwide each year, accounting for over 56% of the total volume produced [6]. Soil erosion has several negative impacts, including a decrease in effective root depth, imbalanced nutrients and water in the root zone, and decreased soil quality.

Furthermore, soil erosion in Morocco may increase the risk of flooding and landslides, which can damage infrastructure and cause loss of life and property. These effects can be particularly pronounced in mountainous regions such as the central High Atlas of Morocco, where soil erosion can be a significant challenge for farmers and communities that rely on agriculture for their livelihoods. In addition to its impact on agricultural productivity, soil erosion can also lead to decreased biodiversity, as it reduces the ability of ecosystems to support a variety of plant and animal life. Thus, addressing soil erosion in Morocco is critical for ensuring the long-term sustainability of agricultural production and the natural environment. These factors reduced agricultural production [7]. In addition, soil erosion causes millions of tons of sediment to reach reservoirs and lakes, damages dam facilities, and has high economic costs due to the negative impact on water quality [8–10]. Therefore, soil erosion is viewed as a significant threat to global economic and environmental sustainability. Both temporally invariable parameters such as lithology and watershed size, and variable factors such as climate, hydrology, ground-cover, and land use impact sediment yield [5,11,12]. Sediment transportation and deposition processes are primarily influenced by four main factors: topography, land use, climate, and soil erodibility. These processes can be aggravated by human activities such as agricultural practices and deforestation [13]. Assessing water erosion in catchments at various temporal and spatial scales is important for preserving and protecting soil and technical constructions such as hydroelectric projects, irrigation dams, and flood attenuation structures.

There are multiple models and methodologies [14–16] that can be utilized to evaluate erosion and sediment production. These models have varying limits of application, incorporate diverse scientific techniques and modeling approaches, and provide output information such as erosion sediment production, sediment transportation, and erosion intensity in high-risk areas. The complexity, considered processes, and data required for calibration and application also differ among the models.

Different models have been used to evaluate soil erosion rates, with modeling being a common tool in erosion studies [17]. These models can be divided into empirical and process-based models. Examples of empirical models include USLE [18], RUSLE [19], MUSLE [20], and modified versions of these models. Process-based erosion models include LISEM [21], MMF [22,23], WATER/SEDEM [24], SWAT [25], WEPP [26], and EUROSEM [27].

The Gavrilović method (Erosion Potential Model) is a method used to assess the potential for erosion on a given site [28–30]. The applicability and simplicity of the Gavrilović method may make it a popular choice in some contexts, but there are many other available erosion models and approaches and the choice of the model may depend on factors such as the specific characteristics of the site including the climate context, topography, and drainage network of the study area, as well as other characteristics. For example, in an arid region with steep slopes and a well-developed drainage network, a model that accounts for high-intensity rainfall events may be more appropriate than a model that assumes a uniform rainfall distribution. Similarly, in a region with a high degree of soil heterogeneity, a model that accounts for variations in soil properties may be more suitable. In areas where vegetation cover plays a significant role in erosion processes, models that account for the impact of vegetation on soil stability may be preferred. Additionally, the availability of data and resources should be taken into account, as some models require more detailed data and computational power than others. Ultimately, the choice of an erosion model should align with the goals of the erosion assessment, whether that is to identify critical erosion areas, predict future erosion rates, or evaluate the effectiveness of erosion control measures.

The EPM method takes into consideration six factors based on surface geology and soil properties (coefficient/erodibility factor (Y)), topographic features (slope (J)), climatic factors (annual rainfall (H), and annual temperature (T)), land use type and distribution (coefficient/soil protection factor (x)), and the catchment's degree of erosion (erosion and stream network development coefficient (φ)). It has been widely implemented in countries, e.g., [15,31–41] and has provided reliable results for evaluating soil erosion severity, estimating mean annual soil loss/sediment yield, and implementing erosion control measures such as torrent regulation.

The Priority Actions Program/Regional Activity Center (PAP/RAC) method, which is the second applied model in this research, is an innovative approach designed for managing Mediterranean coastal areas. It allows for the presentation of erosive states, the dynamics of water erosion processes, and the assessment of risk trends at different scales in a watershed. Many studies have been conducted on water erosion using the consolidated PAP/RAC approach [42–49], which aims to integrate the anthropogenic parameter by analyzing its behavior with the environment. These studies have demonstrated the reliability of the PAP/RAC method using GIS (Geographic Information Systems) and RS (Remote Sensing) technology, which can process spatial data regardless of location and scale [50–57].

The main aim of this study was to assess and compare the spatial distribution of eroded areas in the Toudgha River watershed, using the EPM and PAP/RAC models. The resulting maps generated by the models were validated by comparison to the outcrop to ensure their significance.

The Toudgha River was selected for this research due to its importance as the largest tributary of the Gheris basin, its role in meeting irrigation needs, and its supporting agricultural production in the Tinghir region called the "Toudgha River". The models were implemented in a GIS-based environment, with each parameter represented by a digital layer. This approach was adopted to consider the spatial distribution of the input data and the overall development of the phenomenon in a watershed, resulting in more accurate outputs. The digital maps were extracted from the Toudgha River digital elevation model (DEM), the same from geological and land-use maps, as well as data from available information in international databases (Landsat8 Oli imagery and rainfall data). These digital layers were then overlaid to quantify soil loss in the case study according to several correlation matrices.

2. Materials and Methods

2.1. Study Area

The catchment of the Toudgha River, the major sub-catchment of the Gheris basin, is in southeast Morocco, covering an area of 2318 km^2. It is situated on the south flank of the Central High Atlas (CHA) Mountains, which extend for 700km from southwest to northeast Morocco, and are delimited by the Eastern Anti-Atlas (EAA) chain to the south (Figure 1). The region has a mountainous topography, with a maximum elevation of 2116m above mean sea level and diverse climates ranging from arid to semi-arid. The chosen area is located between the geographical coordinates ranging between 31°51′35″ N, 31°9′14″ N and 5°10′45″ W, 5°57′01″ W. The catchment area has a dense network of rivers and streams, with two main tributaries emanating from the western part of the Toudgha River (Target and Sidi Ali Oubourk tributaries). The lithological context of the area is characterized by predominantly limestone, sandy, and sandy-marly substrate from the Upper Cretaceous period to the lower Jurassic clayey units to the north, and by lithological units such as sandstones, schists, and volcanic units to the south (Paleozoic outcrop of Jbel Saghro), which are soft and prone to water erosion. The climate in the region is Saharian, with dry summers. Rainfall is very irregular and the climatic erosivity tends to increase from south to north in the Toudgha river watershed. Erosion processes in arid areas are complex and can be influenced by various interacting factors, such as erodibility, land use, climate, and topography. In particular, mountainous regions of the Moroccan High Atlas are highly susceptible to erosion due to their steep slopes, sparse vegetation cover, and poorly

developed soils. The combination of these factors can result in high rates of soil erosion, which can cause significant socio-economic damage and threaten soil quality. Moreover, anthropogenic activities, such as deforestation and desertification, can exacerbate erosion processes and further degrade the soil. Soil erosion is a major environmental concern in the southeastern regions of Morocco due to the unique characteristics of these ecosystems. Arid soils are often low in organic matter and vulnerable to wind and water erosion, which can result in soil degradation and loss of productivity. Desertification, a process of land degradation that occurs in arid regions, can further intensify soil erosion by increasing surface runoff and reducing vegetation cover. The impacts of soil erosion can be severe in these arid environments, where agriculture and livestock production are critical for the livelihoods of many people. Therefore, it is crucial to implement sustainable land management practices to mitigate erosion and protect soil quality in these regions.

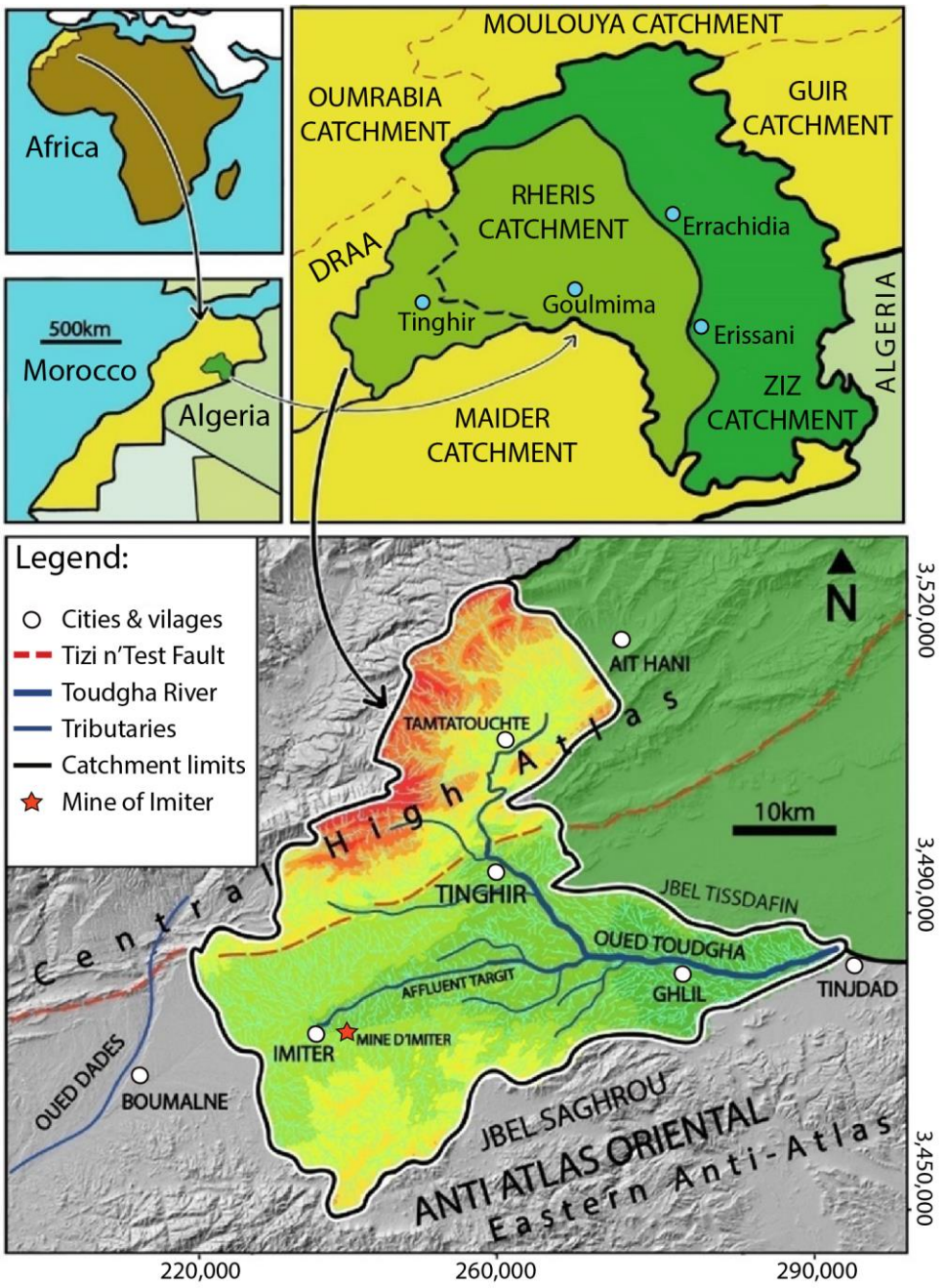

Figure 1. The geographical location of the Toudgha River watershed.

The Toudgha river catchment is located in the western region of the large Ziz-Ghris basin, which is a tectonic depression formed during the Mesozoic era as described by Diani et al. [58]. It is bordered to the north by the Central High Atlas Mountains and to the south by the Anti-Atlas Mountains chain. The Toudgha River is the main tributary in the basin (Figure 1).

It flows from the southern part of the Central High Atlas Mountains (upstream) and the water drainage goes in an east direction (downstream) until reaching the Gheris River at the village of Goulmima. The area is monitored by two hydrological stations: Tamtattoucht, located 20 km north of the Toudgha gorges, and the second named Ait Bouijane, located 40 km south of the first station. The Toudgha River supplies the Tinghir River and then passes through the Tinjdad palm grove before eventually joining the hydrographic system of the Ziz-Rheris basin. The Toudgha River expands downstream and becomes more entrenched in the upstream region. Based on the overall relief depicted in Figure 2a, the basin can be divided into three distinct domains: a high mountain domain featuring high reliefs made up of Liassic-age carbonate facies; an intermediate domain characterized by significant reliefs corresponding to upper Cretaceous hills but with lower elevations than the previous domain, and a downstream domain featuring altitudinal depressions (small sub-catchments) ending in a lowland region occupied by Quaternary deposits. The slopes shown in Figure 2b depict the topographic variations in the Toudgha River watershed steepness, which can be divided into three parts based on their influence on elevation values and flow velocity. The first part is in the northwest and belongs to the Central High Atlas (CHA) mountain range, featuring steep slopes where runoff increased due to the impermeability of the strata (limestone). The second part has medium slope degrees with a low-elevation area derived from the Paleozoic outcrop of the Eastern Anti-Atlas Mountains to the south of the catchment. The third category is located in the central part of the basin and has very low to low slopes, with a non-significant impact on runoff velocity. In summary, the hydrographic slope profile of the entire area can be divided into two main directions shown in Figure 2b, with a steep slope upstream with the N–S main direction leading to stream discharge and sediment production and a second slope direction with low to moderate degrees located from the central part of the basin to the downstream catchment with a W–E direction. The geological setting of the study area includes a variety of units. The oldest deposits, from the Precambrian period, are in the southwest of the basin and consist of sedimentary and volcano-sedimentary series including calco-alkaline intrusions. This entire area has been subjected to low-intensity regional metamorphism. Above these deposits to the north, we found the Paleozoic (Cambrian-Ordovician) lithological units, characterized by sandstone and schist facies, which are predominantly overlain by Mesozoic limestone carbonates (Jurassic and Cretaceous), as described by Diani et al. [58]. The Toudgha River path is surrounded by Tertiary formations, mainly consisting of carbonates that are consolidated limestone and soft to poorly consolidated white-to-purplish sandstone. The recent Quaternary outcrop in the region is made up of alluvial deposits concentrated in the downstream area (Ghelil to Tinjdad villages).

2.2. Methods

The methodology adopted in this study is based on the EPM and PAP/RAC models (Figure 3).

2.2.1. The Erosion Potential Model (EPM)

According to the EPM (also called the Gavrilović method), the annual volume of soil detachment caused by surface erosion is calculated using Equation (1).

$$W = T \times H \times \pi \times \sqrt{Z^3} \times F \quad (1)$$

where W is the average annual sediment production ($m^3/km^2/year$).

T (°C) represents the temperature coefficient, h(mm) is the mean annual rainfall, Z is the erosion coefficient, and F (km^2) is the watershed area.

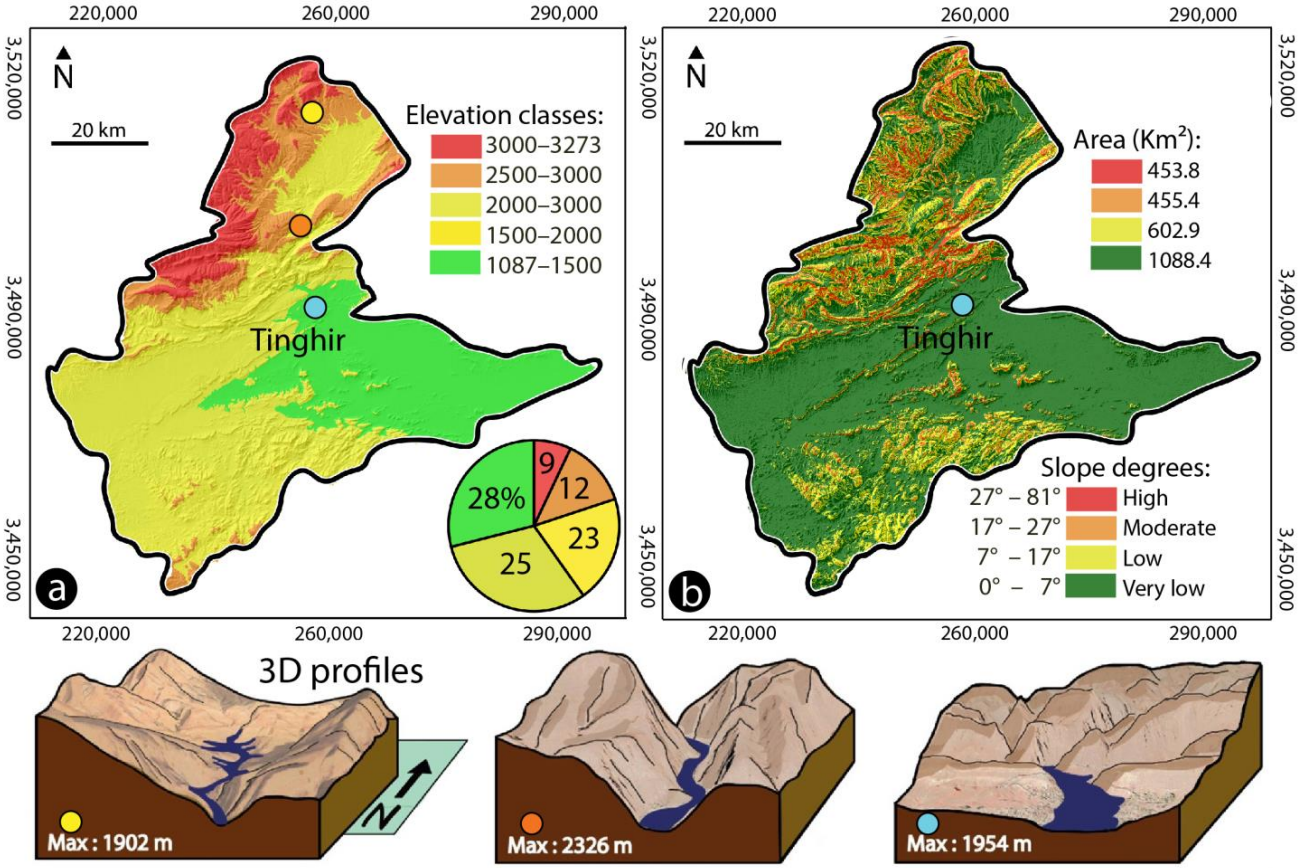

Figure 2. (**a**) Elevation classes and (**b**) slope degrees of the study area.

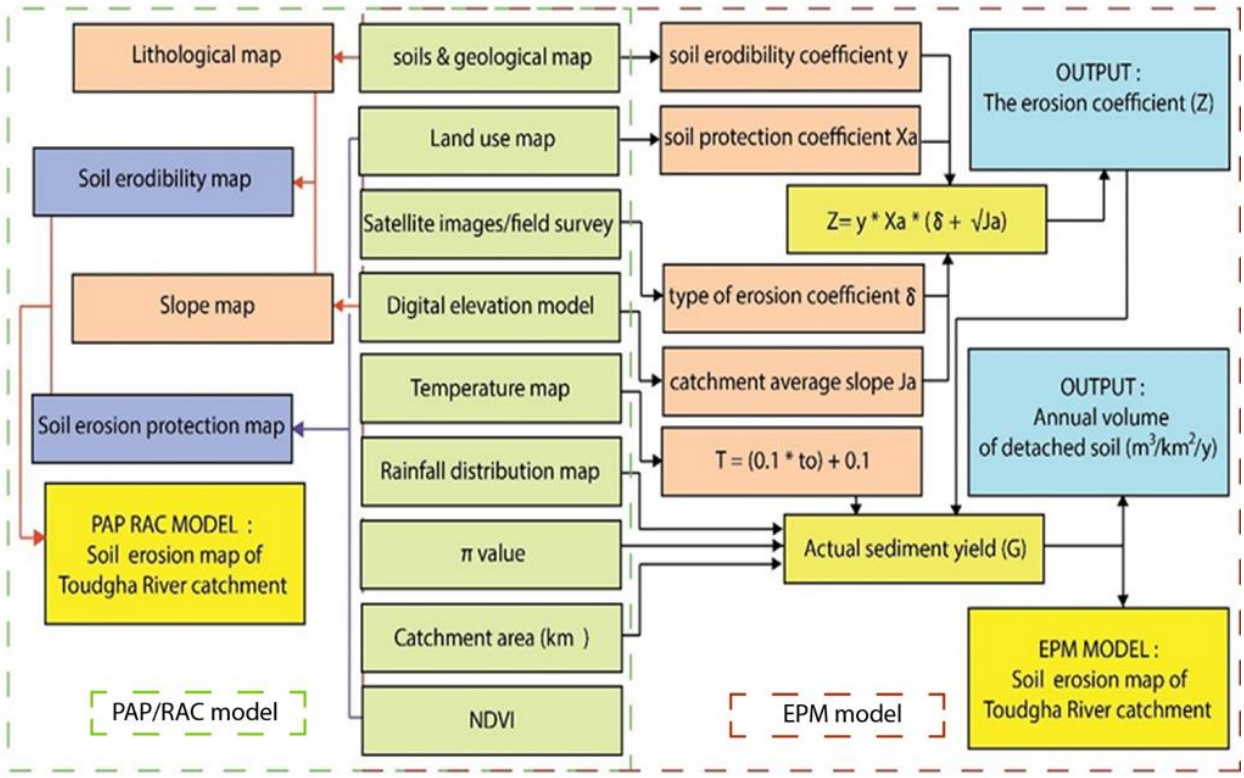

Figure 3. Methodology adopted for running the EPM and PAP/RAC models under GIS software.

The erosion coefficient (Z), which reflects the intensity or density of erosion processes according to [59], is calculated using Equation (2).

$$Z = Xa \times Y \times (\varphi + \sqrt{J}) \quad (2)$$

The erosion coefficient (Z) is a measure of a region's vulnerability to erosion and is calculated based on the soil erodibility coefficient (Y), soil protection coefficient (Xa), coefficient of erosion type and extent (ϕ), and average slope of the area (Ja). Z is the sole output from the method that presents both numerical and descriptive data on the area's erosion susceptibility, as indicated in Table 1.

Table 1. A descriptive evaluation of the EPM model parameters [15,60].

Soil Protection Coefficient (Xa)	**Value**	**Coefficient of Type and Extent of Erosion (ϕ)**	**Value**
Mixed and dense forest	0.05–0.2	Little erosion on watershed	0.1–0.2
Thin forest with grove	0.05–0.2	Erosion in waterways on 20–50% of the catchment area	0.3–0.5
Forest with little grove, scarce bushes, bush prairie	0.2–0.4	Erosion in rivers, alluvial deposits, karstic erosion	0.6–0.7
Damaged forest and bushes, pasture	0.4–0.6	>50% of the catchment area affected by surface erosion	0.8–0.9
Damaged pasture and cultivated land	0.6–0.8	Whole watershed affected by erosion	1
Areas without vegetal cover	0.8–1.0		
Soil erodibility coefficient (Y)	**Value**	**Erosion coefficient (Z)**	**Value**
Hard rock, erosion resistant	0.2–0.6	Excessive erosion >1.00	>1
Rock with moderate erosion resistance	0.6–1.0	Severe erosion 0.70–1.00	0.7–1
Weak rock, schistose, stabilized	1.0–1.3	Medium erosion 0.40–0.70	0.4–0.7
Sediments, clay, and rocks with low resistance	1.3–1.8	Slight erosion 0.20–0.40	0.2–0.4
Fine sediments/soils without erosion resistance	1.8–2.0	Very slight erosion	0–0.2

2.2.2. Erosion Intensity and Sediment Production Assessment Parameters

- Soil erodibility coefficient (Y):

The soil erodibility plays a crucial role in erosion models as noted by several scientists. This coefficient is based on the soil type of the Toudgha River catchment and was derived from four geological maps of the Tinghir and Jbel Saghro regions at a scale of 1:100,000 using the Gavrilović method.

- Soil protection coefficient (Xa):

The soil protection coefficient represents the effectiveness of an area in protecting against erosion and is determined by two independent factors: land use and vegetation cover coefficients. The land use coefficient depends on the type and the characteristics of the land while the vegetation cover coefficient depends on measures taken to reduce erosion, particularly in agriculture. These two coefficients are treated as a single factor in the assessment of soil protection.

Equation (3) [61] used to calculate the Xa parameter in the Toudgha River catchment was:

$$Xa = (XaNDVI - 0.61) \times (-1.25) \quad (3)$$

where:

$$XaNDVI = (\text{NDVI of the catchment specifically with values ranging between } -0.9 \text{ and } +0.6) \quad (4)$$

$$Xa = NDVI\ [(\text{with specific values between} -0.9 \text{ and } +0.6) - 0.61)] \times (-1.25) \quad (5)$$

- Average slope of the study area (Ja):

The slope of the terrain affects erosion by its degree of inclination. This has been demonstrated by several studies [62–67]. An increase in slope enhances run-off, which becomes erosion-prone, and its energy surpasses that of raindrops [1,68]. Also, the distribution of slope classes shows that the low slope class (<20%) is dominant, representing more than 49.3% of the total area, which is concentrated in the intermediate part. Moderate to high slopes represent a percentage of 50.7% for classes over 30%, concentrated in the north and southeast regions.

The AlosPalsar digital elevation model, with a cell size of 12.5 × 12.5 m, was used to determine the average slope (Ja factor) and mean elevation difference (z) of the study area, as well as the perimeter of the study area (O), the length of the principal waterway (Ip), and the drainage density (Dd).

- Coefficient of type and extent of erosion (ϕ):

The map of erosion types was obtained through the overlay of the soil sensitivity to the erosion map and the soil protection degree map based on field observations. The values of the erosion process coefficient of the EPM model were used to determine the "factor (ϕ)" [31]. The erosion process coefficients are classified into 5 categories, ranging from 0.1 to 1.0.

The following equation was used to calculate the coefficient that is integrated into our model (Equation (6)):

$$\Phi = \sqrt{R/Qmax} \quad (6)$$

where R = the band number 4 (B4) in case of using (Landsat8 Oli/Tirs) images.

Qmax = value obtained from the attached MTL file of Landsat images (quantize_cal_max_band_4 = 65,535).

2.2.3. The PAP/RAC Model

The predictive approach involves evaluating and integrating all the factors to establish preliminary hypotheses and gathering data on the present conditions of land degradation based on the potential impact of various parameters that control water erosion (such as slope, lithology, NDVI (Normalized Difference Vegetation Index), soil protection, land use and degree of erodibility). This approach results in elaborating on an erosive states units map, providing a framework for mapping potential soil erosion and general trends. This procedure consists of a series of operations (Tables 2–4).

- Development of the erodibility map:

Two maps of slopes and soils of the catchment (to obtain the erodibility map, the previous maps are overlaid) were created. The slope map and the soils (lithofacies) map of the study area were created using a digital elevation model and geological data, respectively. The slope map was extracted from a Digital Elevation Model provided by the USGS with a resolution of 12.5 × 12.5 m, while the lithofacies map was created by identifying and classifying the various types of rocks, sediments, or soils at the surface based on their cohesion, mechanical resistance, and technical resistance to erosion extracted from geological maps of the area [69]. To address the differences in resolution between maps and satellite imagery, it is important to consider the scale of the map or image. Scale refers to the ratio of a distance on the map or image to the corresponding distance on the ground. For example, we use a medium-resolution satellite image to identify specific features and then use a map to provide additional context and information about the area.

The erodibility factor indicates the ability of a substrate to provide material that can be moved by the erosive force of the rain. The slope is a factor that affects the movement of these materials, as the steeper the slope, the more easily the material can be transported. The erodibility map is created by combining both of the factors (slope degrees with lithofacies categories), and the resulting polygons are arranged according to the matrix (Table 2). The

slope plays a significant role in the amount of runoff and, therefore, the potential for water erosion. Runoff is more likely to occur on steeper slopes, and the amount of material eroded is also typically higher. However, runoff is unlikely to occur on slopes with a gradient of less than 2%. Between 2% and 5%, runoff is possible under certain conditions, such as during a storm or on soils that do not filter water effectively.

Runoff occurs on soils with a slope greater than 5%, and it becomes even more accelerated on slopes greater than 10%. There are two possible explanations for this phenomenon. The first is that the increased slope leads to an acceleration of runoff and the second is that on low-sloped terrain, a layer of water can partially protect soil particles from the "splash effect", which is not present on steeper slopes. These hypotheses were proposed by Alexakis et al. [70] and further explored by Cerdan et al. [71].

Table 2. Correlation matrix of resistance to erosion and slope degrees according to PAP/RAC model.

Degrees	Code	Factor 1 (Slopes Degrees)			Factor 2 (Resistance to Erosion)		
		Classes	Area (km^2)	(%)	Classes Degrees	Area (km^2)	(%)
Very low	1	3–0%	962.3	41.51	Highly resistance	189.58	8.18
low	2	12–3%	554.42	23.91	Medium resistance	371.01	16.00
Medium	3	20–12%	424.74	18.32	Low resistance	436.73	18.83
High	4	35–20%	296.12	12.77	Coarse sediments	456.82	19.70
Very high	5	>35%	80.72	3.48	No resistance	864.6	37.29
		Resistance to erosion					
5	4	3	2	1			
2	1	1	1	1	1		
3	3	2	1	1	2	Slope degrees	
4	4	3	2	2	3		
5	5	4	3	3	4		
5	5	5	4	4	5		

Table 3. Correlation matrix of vegetation density and land cover according to PAP/RAC model.

Degrees	Code	Factor 3 (Vegetation Density)			Factor 4 (Land Use/Cover)		
		Classes	Area (km^2)	(%)	Classes Degrees	Area (km^2)	(%)
Very low	1	<25%	577.92	24.93	Dry plantings	521.84	27.56
Lo	2	25–50	1463.22	63.12	Regular implants	495.25	21.41
Medium	3	50–75	250.12	10.79	Irrigated crops	463.88	20.05
High	4	>75%	27.05	1.17	Forest	369.79	10.98
Very high	5				Dense trees	462.68	20.00
		Vegetation density					
4	3	2	1				
4	4	2	5	1			
4	4	5	5	2	Land cover		
1	1	2	3	3			
1	2	3	4	4			
2	3	4	5	5			

Table 4. Correlation matrix of surface susceptibility to erosion and soil protection according to PAP/RAC model.

Degrees	Code	Erodibility			Soil Protection		
		Classes	Area (km^2)	(%)	Class	Area (km^2)	(%)
Very low	1	Very low	606.33	26.21	Extremely low	136.93	26.21
Low	2	Low	741.8	32.06	Insufficient	300.14	32.07
Medium	3	Medium	500.93	21.65	Average	291.89	21.66
High	4	High	309.27	13.37	Excessive	398.84	13.37
Very high	5	Very high	155.24	6.71	Valuable	1185.42	6.71
		Erodibility					
5	4	3	2	1			
2	2	1	1	1	1		
4	3	2	1	1	2	Soil protection	
4	4	3	2	1	3		
5	5	3	3	2	4		
5	5	4	3	2	5		

- Development of the soil protection map:

Vegetation cover can protect soil from erosion by reducing the energy of erosive agents and by intercepting raindrops with the aerial parts of plants, which can reduce the energy of rain erosion [72]. On the ground, vegetation can also prevent runoff by increasing water infiltration. The protective effect of the latter may vary depending on the type of vegetation or land use [73]. A soil protection map can be created by overlaying the maps of land use with vegetation cover density, and this output map can provide information on the distribution and intensity of vegetation in a watershed. The degree of soil protection in the Toudgha River catchment is determined by applying the matrix (Table 3). Separating the land use map from the coverage density may not be as effective in producing significant results, but combining them can help in identifying areas in need of urgent intervention.

After developing the maps of land cover and vegetation density of the catchment and obtaining the protection map, the previous factors were overlaid. The land cover map was created from the Landsat 8 satellite imagery with an acquisition date of the year 2019, which was provided by the United States Geological Survey (USGS) [73] by using a supervised classification process with ENVI software, and it shows the different types of land cover in the area [74,75]. The second map of vegetation cover density was created by calculating the NDVI (Normalized Difference Vegetation Index). The two previous factors were then classified based on percentage values and recommendations from the PAP/RAC model [76] (Table 3).

- Overlying the erodibility and the soil protection maps:

The mapping of erosive states of the study area was carried out by overlaying the erodibility and soil protection maps (data from correlation matrices of Tables 2 and 3). The assessment and mapping of soil sensitivity to water erosion typically involve identifying indicators that can help locate erosion risks in space and time [77]. This is typically achieved using observations or measurements [78]. The methodology adopted in this case is based on the PAP/RAC third correlation matrix (Table 4), which combines information about the physical state of the soil (such as topography and lithofacies) with the protection provided by vegetation cover and land use type. This approach allows for a good estimate of susceptibility to erosion in a specific area.

2.2.4. Causal Factors

The water erosion sensitivity of an area can be mapped using various impact factors. These factors include the lithologic unit, elevation, slope degrees, the NDVI (Normalized Difference Vegetation Index), land use, and rainfall. The lithologic unit refers to the rock type or soil composition of the area. Elevation determines the steepness and height of the land, affecting the speed of water flow. Slope degrees also contribute to the speed and direction of water flow, as steeper slopes increase the erosion potential. The NDVI measures the amount of vegetation in the area, with higher values indicating less erosion potential. Land use affects the level of soil disturbance and vegetation cover. Lastly, rainfall determines the amount and intensity of water that impacts the area, influencing erosion potential. By considering all of these factors together, researchers can create a comprehensive map of water erosion sensitivity for a specific area.

- Lithology, or the physical and chemical characteristics of rock, plays a significant role in the erosion of water [79]. The type of rock can also influence the rate at which erosion occurs. For example, sandstone is more porous and, therefore, more susceptible to erosion by water than a denser rock like basalt. Understanding the lithology of an area can help predict the erosion patterns and the potential impacts on the surrounding landscape. The lithological formations had been extracted from four geological maps of the area. The sediments and rocks within the basin vary in age from the Precambrian to Quaternary periods (Figure 4a).
- Land use/cover, or the type and density of vegetation and other surfaces on the land, can have a significant impact on water erosion [80,81]. For example, areas with high levels of vegetation cover experienced less erosion than areas with low vegetation cover. This is because vegetation intercepts and slows down the flow of water, reducing the energy of the flow and decreasing the likelihood of erosion. In addition, vegetation can help stabilize the soil by rooting into the ground and holding it in place. On the other hand, areas with bare soil or impervious surfaces, such as asphalt or concrete, are more prone to erosion because the water flows more quickly and with greater energy over these surfaces. The land use of the Toudgha catchment was used to prepare the thematic layer (Figure 4b) and then reclassified into three categories: soils or soft sediments, hard rocks or substratum, and vegetation classes.
- Rainfall is a major factor that influences water erosion. The intensity, duration, and frequency of rainfall events can all affect the erosion process [82–84]. High-intensity rainfall events, which have a shorter duration but a higher rate of precipitation, are more likely to cause erosion than low-intensity events. The higher intensity of the rainfall increases the energy of the flow and the likelihood of erosion. Annual average precipitation for the Tinghir province was categorized into three classes: 400–500, 500–600, and 600–700 mm (Figure 4c,d).
- The NDVI (Normalized Difference Vegetation Index) is a remote sensing tool that measures the greenness of vegetation. The NDVI can be used to assess the impact of vegetation on water erosion. For instant, Merritt et al. [14] found that areas with high NDVI values, indicating dense vegetation cover, experienced less erosion than areas with low NDVI values, indicating sparse vegetation cover. This is because vegetation intercepts and slows down the flow of water. The NDVI can also be used to monitor changes in vegetation cover over time and assess the potential impacts on erosion. In Mediterranean catchments, erosion increased as NDVI values decreased. In our case study, the NDVI was reclassified into three classes: (a) (<−0.23), (b) (−0.23–0.26), and (c) (>0.26–0.7) (Figure 4e).
- Slope, or the angle of the land surface, can have a significant impact on water erosion. In general, steeper slopes are more prone to erosion than moderate slopes because the water flows more quickly and with greater energy over steep slopes. Understanding the relationship between slope and erosion is important for predicting erosion patterns and the potential impacts on the surrounding landscape [84]. The slope map of the

Toudgha River catchment (Figure 4e) was divided into five slope categories: (a) (0–7°), (b) (7–16°), (c) (16–27°), (d) (27–81°).

- The elevation is a factor that is frequently used in research on flood and erosion susceptibility because it is a predisposing parameter that is influenced by various geologic and geomorphological processes [74,75]. In the Toudgha River watershed, an elevation map was created using a digital elevation model, showing that the elevation values in the area range from 1332 to 3273 m and can be divided into five classes: 1087 to 3272 m, 1087 to 1462 m, 1462 to 1733 m, 1733 to 2061 m, and 2061 to 3273 m (Figure 4f).

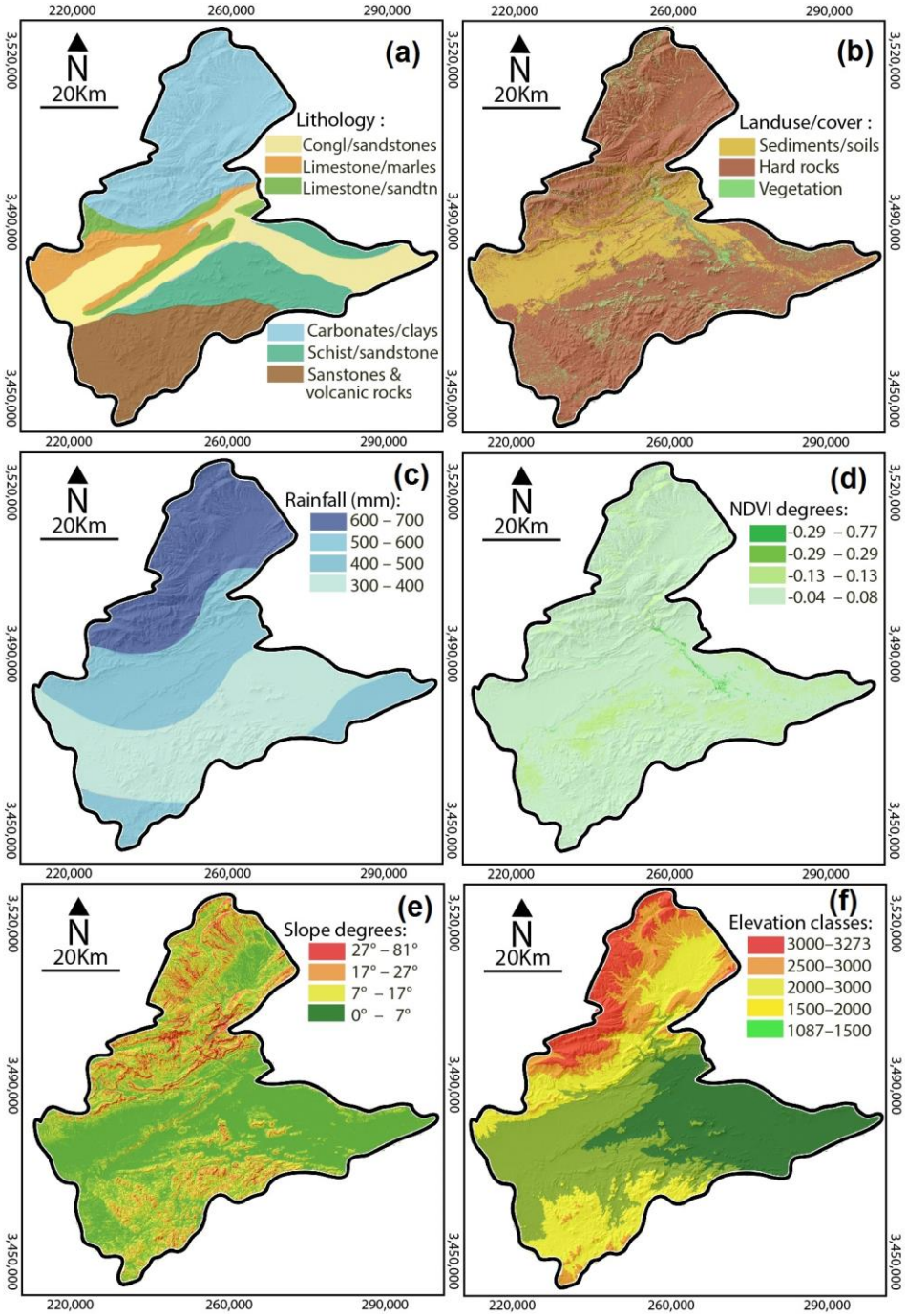

Figure 4. Causal factors of the erosion involved: (**a**) lithological units, (**b**) land use, (**c**) rainfall, (**d**) NDVI, (**e**) slopes, and (**f**) elevations.

3. Results and Discussion

3.1. PAP/RAC

According to the results of the modeling (Figure 5a), the distribution of erodibility in the Toudgha River watershed is influenced by the slope and the cohesive properties of the lithological facies. Using the PAP/RAC approach, areas with steep slopes and low resistance are always highly erodible. The strong and very strong erodibility classes are in the upstream and followed by southern parts of the watershed, where the slope is greater than 30%. The low and very low erodibility classes are found in the center and downstream parts of the catchment, where the slope is weaker. The most common classes are those of moderate, average, and extreme erodibility, which make up 28.69%, 16.72%, and 18.64% of the total area, respectively. In summary, the cohesive properties of the soil and the characteristics of the slopes significantly impact erosion at the watershed level. Steep slope areas tend to have soils with low resistance and high erodibility (Figure 5a).

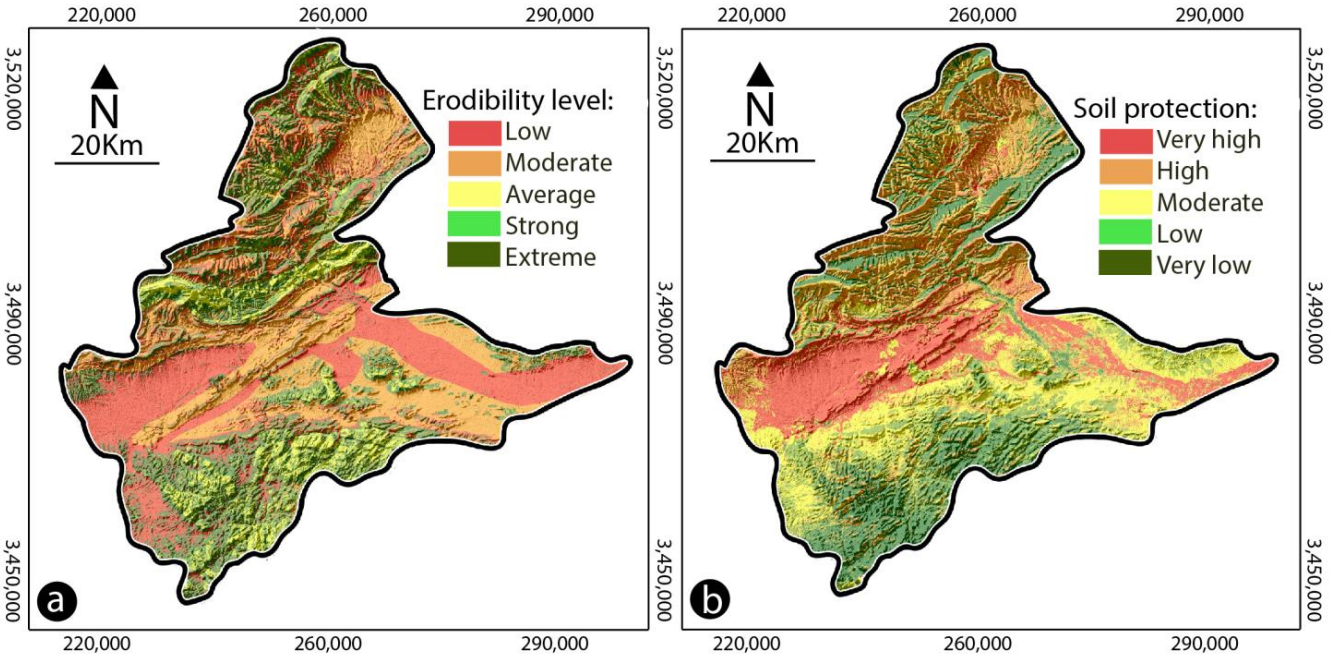

Figure 5. Maps of erodibility (**a**) and soil protection (**b**) according to the PAP/RAC approach.

From the analysis of the soil protection output map (Figure 5b), the Toudgha catchment has poor protection mainly in high-elevation regions (Central High Atlas and Jbel Saghro). The most common areas have weak protection (very low and low classes), which covers 56.34% of the total area and is found throughout the basin, particularly in the upstream and southern parts of the watershed. Even areas near rivers are not well protected; the medium protection class covers 15.72% of the total area, while the very high protection occupies 27.94% of the total protection degree located in the western region. The agricultural fields in the Toudgha River are limited to cereal crops and rely on the often-poor rainfall in the region which makes it more protected from erosion. Vegetation cover provides only weak protection for the soil in limited areas and reforestation is limited due to the lack of irrigation waters. The abundant categories of trees in the region are olive and palms with small leaves and little groves which provide medium soil protection. Degraded lands and the vicinity of the Toudgha River and its tributaries of Oued Target and Oued Ichem become sterile due to erosive processes such as surface gullies and widespread gullying, mainly in villages such as Imiter, Timadrouine, Toulouine, Ouaklim, Ghelil, and Tinjdad.

3.2. Erosion Potential Model

Characteristics of factors governing erosion in the Toudgha River watershed:

The intensity of soil degradation is the result of the combination of several factors (natural and anthropogenic) and their magnitude and classification according to the matrices defined by Gavrilovic [28,29] are presented in the following paragraphs.

Sensitivity of lithological formations to erosion (Y):

It is indispensable that the nature of lithological formations plays a very important role in the amplification of erosion. Indeed, our study basin is characterized by the dominance of sandstones, clay, and marly rock units, which are very sensitive to the action of water and erosive processes. Thus, more than 50% of the total area of the catchment is composed of classes whose sensitivity is low to moderate (0.24 to 0.40) (Figure 6a).

Protection by vegetation cover (land use) (Xa):

The role of vegetation cover in mitigating the action of erosive agents is well established and demonstrated by numerous studies. Indeed, vegetation reduces the velocity of runoff and decreases the kinetic energy of raindrops. However, its protective power is largely influenced by the dominant species and the rate of coverage. The Toudgha River watershed is characterized by a certain variety of vegetation formations, but their densities are not sufficient to provide adequate soil protection, mainly in the northern parts with more than 75% of the area of the basin characterized by low vegetation cover protection (Figure 6b).

Slopes (Ja):

The study area is marked by the presence of steep to very steep slopes in the upstream region. This relief configuration is favorable to runoff; it leads to a rapid movement of water from precipitation and increases the amount of water volume that runs to the downstream level. These slopes provide high erosive power by water and promote an increase in the rates of eroded materials from the upstream to the downstream of the catchment (Figure 6c).

Erosive state (Φ):

The erosive state varies depending on the distribution of the intensity of agents involved in erosion, namely, vegetation cover, lithological formations, slope, climate, and land use. The values of the erosive state in our basin (Figure 6d) range from 0.01, where erosion is low, to 1.05, where erosion is strong. Indeed, more than 70% of the area of the basin is marked by a moderate to very strong erosive state (between 0.43 and 1.05).

The erosion coefficient (Z) is the basic value for all EPM calculations [28,29,31]. This coefficient has been used to separate the intensity of erosion into classes or categories. The overlying of the four used factors, Ja, Y, Xa, and Φ, allows the determination of the potential erosion intensity Z (Figure 6e). Therefore, the differentiation of areas highly affected by erosion (unstable zones) from areas less affected (stable zones or environments where the intensity of erosion is relatively low) were as follows:

Zones where erosion is very weak to moderate occupy more than 65% of the basin's surface and they are aligned with areas of strong protection by vegetation cover, low land, and high resistance of lithological formations.

Areas marked by strong to very strong erosion occupy an average of 35% of the whole area. These regions show a great extent of erosive potential in our study area as it is the result of the combination of the dominance of soft lithological units, weak protection by vegetation cover, and the presence of steep slopes.

Rainfall and temperatures:

Precipitation plays a very important role in erosive dynamics; it directly contributes to the onset of runoff and material transport. The duration and intensity of precipitation are decisive in determining or evaluating the quantities of eroded materials. In the Toudgha River basin, the upstream-downstream variations of precipitation (between 300 and 700 mm) and their spatio-temporal intensities promote the removal of considerable amounts of materials. The EPM model integrates temperature as a factor in the quantitative evaluation of water erosion. There are no values related to this climatic element derived from observations or instrumental measurements in the watershed. Surface temperatures from satellite images were considered. These show large spatio-temporal variations at the scale of the watershed, introducing an additional dimension in the spatial variation of water

erosion in the Toudgha catchment. Thus, the characteristics of all the generating, regulating, and accelerating factors of erosion give the study area a moderate to high fragility and intense vulnerability to the triggering and extension of water erosion.

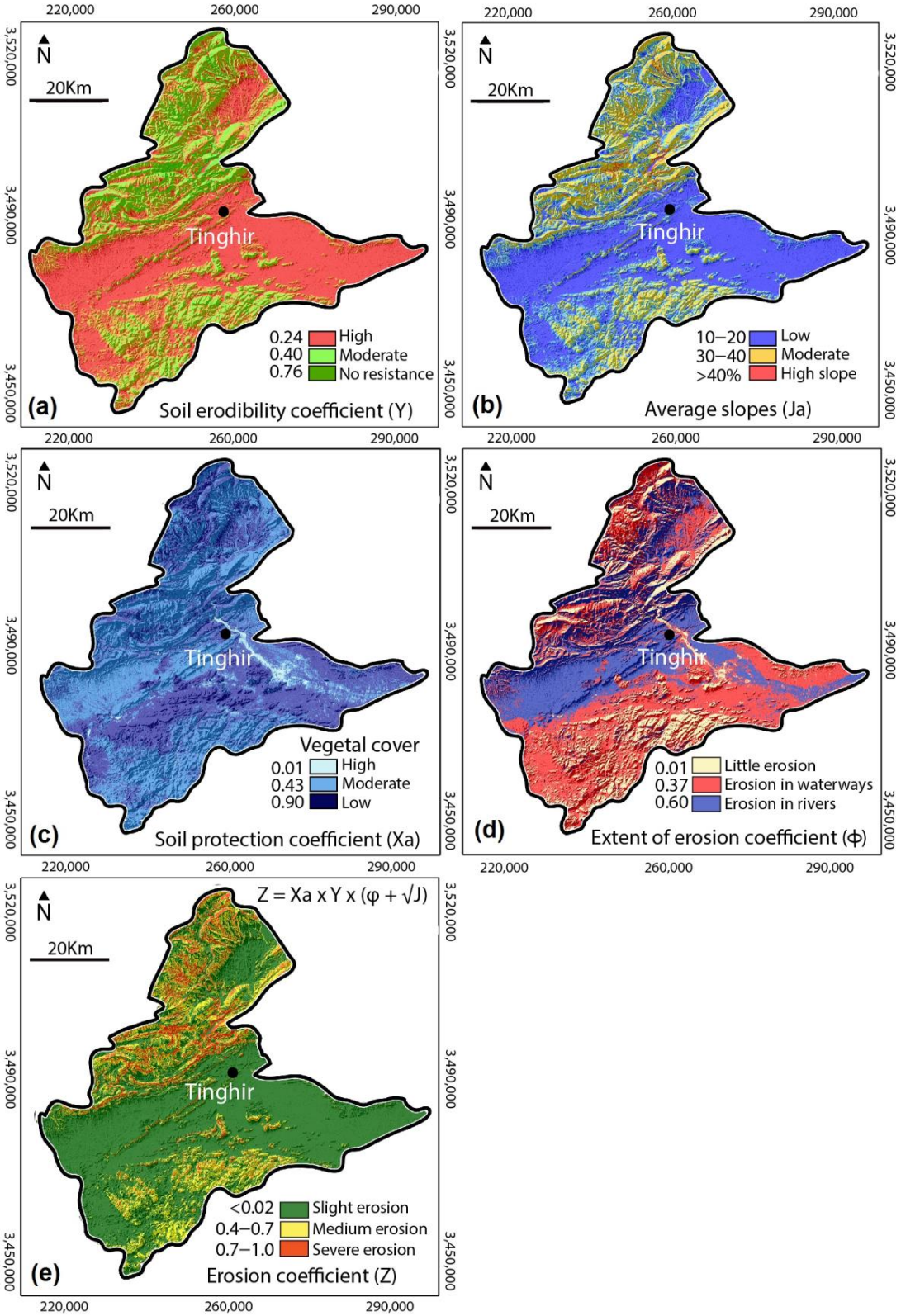

Figure 6. Digital maps of the EPM model parameters (**a**): Y factor; (**b**): Xa factor; (**c**): Ja factor; (**d**): Φ factor; (**e**): the erosion coefficient Z of the Toudgha River catchment.

Synthetic maps of the models:

The comparison aims to validate the geographical location of detected vulnerable areas, and then it is important to compare both the location and degrees of erosion. While EPM quantitative (erosion rate) and PAR qualitative (level of erosion) data may provide different types of information, both can be used to assess erosion and validate the location of vulnerable areas. EPM quantitative data can provide information on the erosion rate over time, while PAR qualitative data can provide a snapshot of the current level of erosion at a specific location. By comparing both types of data, it is possible to identify areas with a high erosion rate as well as areas with a high level of erosion, which can help to validate the location of vulnerable areas as well as the final maps. It is important to note that while EPM and PAR provide different types of data, they are both important tools for assessing erosion and can be used in conjunction with one another to provide a more comprehensive understanding of erosion patterns.

According to the final map of the EPM model (Figures 7 and 8), the highest amounts of soil loss occurred in the Toudgha River catchment are located in the northwest, with an average of 4000 $m^3/km^2/y$. This area has the highest amount of rainfall and snowfall throughout the year, mainly during the winter season as well as marly, dolomite, clay, and sandstone lithological units. The steep slopes and low vegetation cover of this area make it a highly susceptible source to water erosion and floods (Figure 9), including falls, topples, translational slides, and lateral spreads. Based on the spatiotemporal analysis of potential soil loss from water erosion in all parts of the area, we can conclude the following results (Figure 7a): 40.62% of the catchment area (about 940.26 km^2) had a significant soil erosion rate, defined as less than 800 $m^3/km^2/y$. This area was characterized by a dense vegetation cover (Toudgha River) and low slope degrees (lowlands), as well as concentrated urban building. A total of 16.72% of the area (386.74 km^2) had a moderate soil erosion rate, with an annual erosion of (2000–3000 $m^3/km^2/y$), this area is located in the south region and has a medium slope degree, which belongs to the Anti-Atlas Mountains. A total of 42.66% of the area (986.98 km^2) had the highest soil erosion rate (severe and excessive classes), with an average erosion rate equal to 3000 $m^3/km^2/y$ of soil loss. This area was identified as a high-risk region due to moderate to steep slopes, moderate to high vegetation cover, and is characterized by degraded lands.

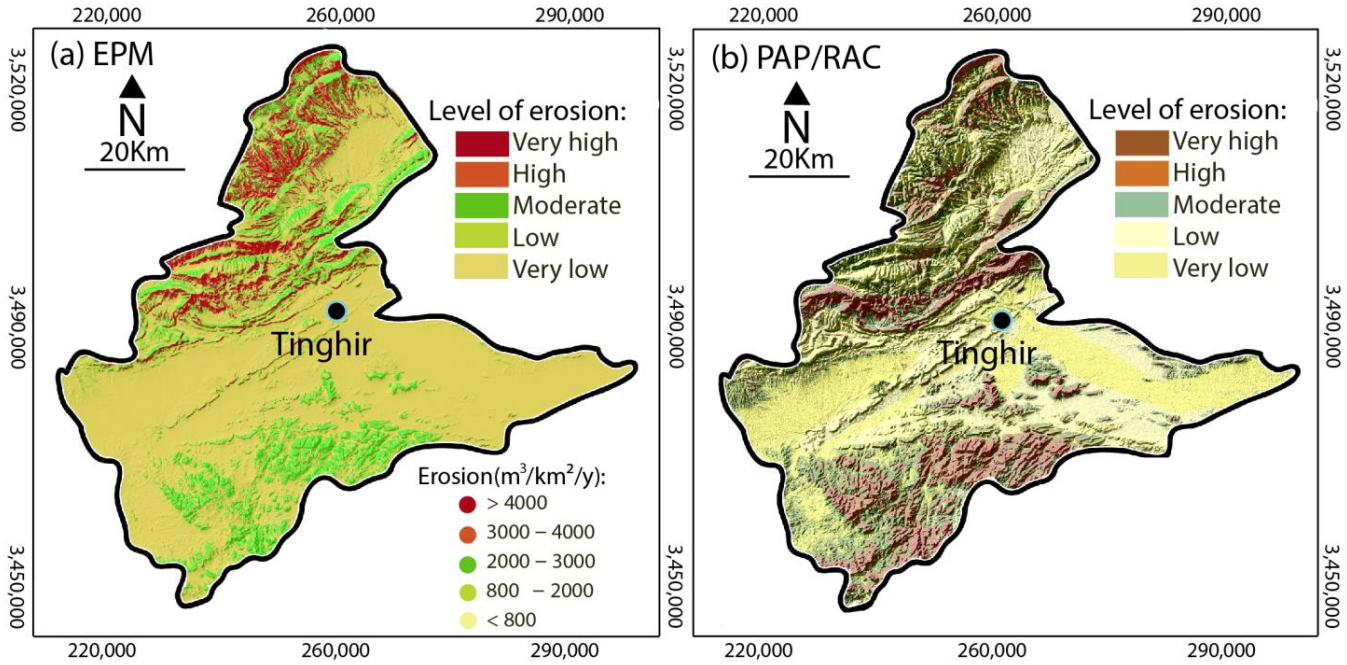

Figure 7. Maps of potential erosion risk of Toudgha River catchment. (**a**) EPM model and (**b**) PAP/RAC model.

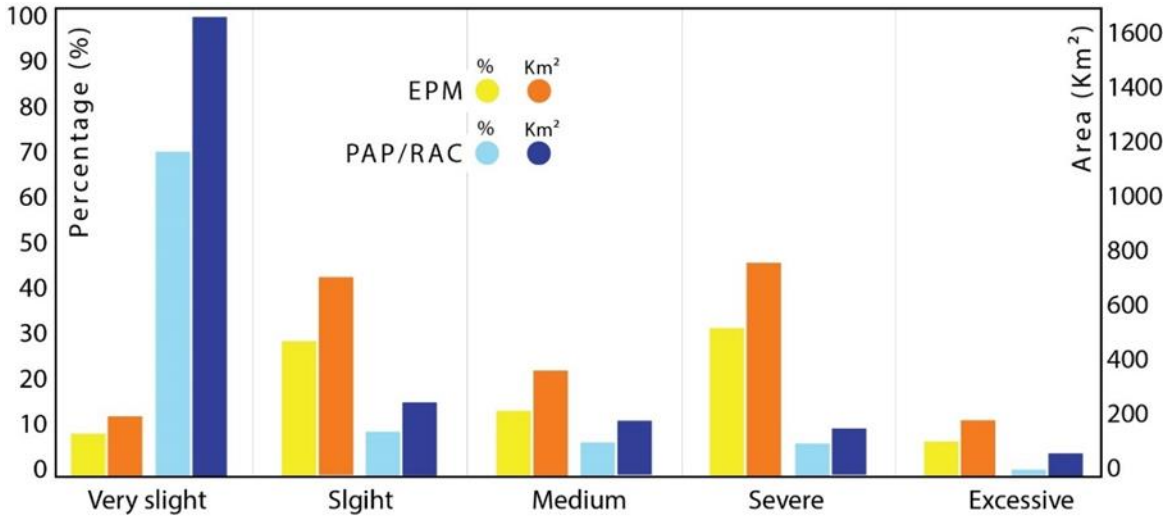

Figure 8. Evolution of impacted areas regarding the erosion degrees of both prediction models.

Figure 9. Photographs showing the severity of water erosion and associated floods in the study area: (**1**) Taghia, (**2**) Taghzout, (**3**) Ait Iala, (**4**) Ait Hani, (**5**) Tilouine, (**6**) Taghia, (**7**) Asfalou, and (**8**,**9**) Tizgui.

The PAP/RAC model provides a synthetic map of soil erosion distribution (Figures 7 and 8), which demonstrates that the Toudgha River catchment is highly susceptible to erosion, mainly in the upstream region. The catchment can be divided into five classes of sensitivity, with the percentage of each class as follows: very low (71.57%), low (10.93%), moderate (7.85%), high (2.67%), and very high (6.97%) erosion sensibility of the total catchment area (Figure 7b). Areas with the highest vulnerability to erosion (classified as very high sensibility) cover a total of 9.65% of the whole catchment and are located in the extremity of the northwestern part, the vicinity of the Tizi n'Test fault to the south of the watershed (Jbel Saghro outcrop). These areas are characterized by soft and non-cohesive rocks, lack of vegetation cover, steep slopes, and weak resistance to weathering. In contrast, the central part of the basin, covering around 185.27 km^2, which is equal to 7.85% of the whole catchment area, has shown moderate slope degrees, high to very high soil protection, and medium erodibility, demonstrating fewer erosion rates compared to the north and south regions. The remaining region is classified as having low to very low levels of erosion, covering a total of 82.50% of the area and having well-protected soils consisting of compact and unaltered rocks, which are located mainly in the western part (downstream) and characterized by adequate vegetation cover (Toudgha River), well-draining soils, lowlands, and reforestation activities. By using PAP/RAC mapping and considering factors such as slopes, geological data, land cover, and vegetation cover, it was possible to describe the state of erosion in the Toudgha catchment and identify areas where erosion sensitivity is high. The reduction in vegetation covers due to both climatic conditions and human activities, such as overgrazing, is a significant factor contributing to erosion in the study area. To reduce soil loss and control water erosion in the catchment, various measures can be taken, including reducing grazing pressure, reforestation, and using check dams to control surface runoff. These solutions will help to protect the soil and riverbanks and enhance the sustainability of the ecosystem in the Toudgha River catchment.

Both models used in this study confirmed that the north and south regions are the most vulnerable (characterized by high erodibility and low soil protection degrees), which is consistent with the field observations in the study area (Figure 9). These regions are distinguished by high elevation, steep slopes, intense rainfall, low vegetation density, fragile rock formations, the density of fractures and faults, and rapid topsoil erosion. Based on their high susceptibility to erosion, these regions should be given priority in terms of mitigation and maintenance efforts [85]. One of the main limitations of this study is the diversity and resolution of the data sources used, including DEM, LULC, lithology, and soil types (Table 1). It is challenging to choose the appropriate spatial resolution in natural hazard modeling studies, as pointed out by Elbadaoui et al. [86]. This issue is particularly relevant in areas with limited geographical data, such as the southeast of Morocco. To conduct this study, all the thematic layers were resampled at a 12.5 m resolution. Another limitation is the lack of data on important parameters such as soil texture, soil depth, and water table depth. Despite these limitations, the results of this study can still be considered effective for improving the quality of spatial outputs related to water erosion prediction at the national level, as demonstrated by the performance evaluation. In summary, the results of the field validation of the EPM and PAP/RAC models for estimating erosion potential in the Toudgha catchment showed that the locations of moderate and heavy erosion potential were accurately predicted, while the locations of slight erosion potential were not as accurate. The EPM model provided more reliable results compared to the PAP/RAC model, with both models yielding similar and generally reasonable results concerning field evidence.

To control erosion in these areas, several solutions can be implemented. One approach is to improve vegetation cover, which can protect the soil from erosion by stabilizing the surface and absorbing excess water. Other methods include the use of physical barriers, such as fences and terraces, to slow down water runoff and control sediment transport. Additionally, sustainable land use practices, such as conservation tillage and crop rotation, can help to reduce soil erosion and improve soil health.

Compared to other desert regions in North Africa, the areas in the table data share similar characteristics and erosion patterns. For instance, the High Atlas Mountains region, which covers parts of Morocco, Algeria, and Tunisia, is characterized by steep slopes, low vegetation cover, and frequent rainfall and snowfall during winter seasons, similar to the areas in the EPM and PAP/RAC models. The Sahara Desert region, which spans several North African countries, is also prone to erosion due to its arid climate, wind erosion, and dune movement.

The qualitative study of potential erosion using the PAP/CAR method, based on natural factors (slope, lithology, vegetation cover, and land use) allows for the analysis and understanding of the issue of erosion risk in the study area. It demonstrated its importance as an effective tool for a simple and rapid general diagnosis of potential hydraulic erosion risk at the watershed scale of the Toudgha River. This work enabled the establishment of a multi-source database on the study region and demonstrated the importance and contribution of geographic information systems and remote sensing to the mapping of areas at risk of hydraulic erosion. The predictive phase provided information on the current state of soil degradation based on the degree of influence of different factors that control hydraulic erosion. It shows that 80.52% of the studied watershed has low to moderate erodibility, while only 19.48% has high to very high erodibility. The descriptive approach showed that soil degradation and loss manifest in different forms of hydraulic erosion, with a predominance of gullies and surface rills in low lands downstream, as well as sheet erosion in the central part of the catchment.

The model outputs of the EPM rely heavily on the multiplication of the model parameters. As an example, when the average erosion resistance of rocks (soil erodibility coefficient Y) varies, the total annual volume of detached soil (Wa) will vary proportionally. However, not all parameters are included in the model through multiplication. Some parameters such as the average slope of the study area (Ja), average annual temperature (T0), and drainage density (Dd) are categorized as high-sensitivity factors. The multiplication-form parameters are classified as very high-sensitivity factors. During model modification, it is essential to consider two things to reduce model errors and uncertainties. Firstly, it is necessary to assess whether the average annual temperature is given sufficient significance in the model. Secondly, it is important to evaluate whether the integration of T0, which represents the annual temperature average (e.g., 32° for the Tinghir region in our case) in the model, limits its applicability to regions with similar climates.

The topography of the upper part of the Toudgha River catchment, specifically the average slope length and gradient, significantly influences water erosion, runoff, and downslope sediment transport. The parameter representing these characteristics, Ja, has a high impact on the model outcome. However, when considering its sensitivity index, I, Ja falls within the lower high-sensitivity class values.

In a previous study by Elbadaoui et al. [86], it was found that the ranking of parameter sensitivity is dependent on the variable, location, and case study. Therefore, it is necessary to conduct a sensitivity analysis for each new catchment study to select a subset of parameters for model calibration and uncertainty analysis. The most sensitive parameters identified in the sensitivity analysis for the Gavrilović method are also considered significant in the scientific literature on erosion analysis [28–30].

Specifically, the soil erodibility coefficient and soil protection coefficient Xa are classified as very high-sensitive parameters, with Xa being a high-sensitive parameter concerning the Wa model output. In a separate analysis [28,29], the effect of using different information sources for the land use parameter Xa was investigated, revealing significant deviations in model output values. This analysis not only explores parameter uncertainty in the model but is also closely related to parameter sensitivity analysis since both consider deviations in parameter values, whether intentionally chosen or defined by external factors.

The results from the different degrees of erosion for the EPM and PAP/RAC models highlight the need for effective erosion control measures in these arid areas. Factors such as wind erosion, water erosion, and soil compaction contribute to erosion, and solutions

such as improving vegetation cover, using physical barriers, and implementing sustainable land use practices can be effective in controlling erosion. The characteristics of these areas are comparable to other desert regions in North Africa, emphasizing the importance of studying and implementing effective erosion control measures in these regions. In summary, model parameterization plays a crucial role in determining the accuracy of model outputs. The sensitivity of each parameter should be carefully evaluated, and modifications should be made accordingly to reduce errors and uncertainties. Additionally, the applicability of the model should be assessed to ensure that it can be used in various regions and environments [87,88].

4. Conclusions

Soil erosion is a significant environmental issue that can result in reduced agricultural productivity, increased sedimentation of waterways, and loss of biodiversity. The north of the Toudgha River catchment located in the southeastern region of the Central High Atlas is particularly susceptible to erosion due to unfavorable erosion factors, mainly steep slopes, soft rocks, and low vegetation cover.

To address this issue, this study utilized a range of tools to provide a comprehensive understanding of erosion mapping. The EPM showed that annual estimating and the sensitivity of soil loss varied from upstream to downstream of the catchment due to differences in erosion factors and changes in vegetation cover resulting from land management and climate change. Meanwhile, the PAP/RAC method provided the distribution of soil loss over the catchment based on physical properties and protection factors. The results indicate that the upstream region of the Toudgha catchment with 9.65% and 8.56% of the whole area is highly or very highly prone to water erosion by applying both PAP/RAC and EPM, respectively. The correlation of the results between the two models highlights the importance of considering the quality of the user data, the climatic characteristics of the chosen area, and determining the number of coefficients for each model.

The information generated from this case study can be utilized in natural resource and soil conservation projects to develop targeted strategies for erosion control and prevention in the south of the High Atlas regions. However, it is important to recognize the limitations of the EPM and PAP/RAC methods, which rely heavily on expert knowledge and experience, and that further research is needed to refine their accuracy and explore their effectiveness in other regions. In conclusion, this study provides valuable insights into the severity of erosion in the Toudgha River watershed and emphasizes the importance of employing a range of tools and approaches to comprehensively analyze soil erosion. This knowledge can help to inform future conservation and management efforts, ultimately leading to a more sustainable and resilient ecosystem.

Author Contributions: Conceptualization, K.E., S.M., M.I. and M.A.; methodology, K.E., S.M., M.I. and M.A.; software, K.E., S.M. and M.I.; validation, M.I., K.A., T.A.-A. and M.A.; formal analysis, K.E., S.M., M.I., K.A., T.A.-A. and M.A.; investigation, K.E.; resources, K.E.; data curation, K.E.; writing—original draft preparation, K.E., S.M. and M.I.; writing—review and editing, K.A., T.A.-A. and M.A.; visualization, M.I. and M.A.; project administration, M.A.; funding acquisition, K.A. All authors have read and agreed to the published version of the manuscript.

Funding: This research was funded by the Researchers Supporting Project, number RSP2023R351, King Saud University, Riyadh, Saudi Arabia.

Data Availability Statement: The data presented in this study are available upon request from the corresponding author.

Conflicts of Interest: The authors declare no conflict of interest.

References

1. Jain, M.K.; Das, D. Estimation of sediment yield and areas of soil erosion and deposition for watershed prioritization using GIS and remote sensing. *Water Resour. Manag.* **2010**, *24*, 2091–2112. [CrossRef]
2. Issaka, S.; Ashraf, M.A. Impact of soil erosion and degradation on water quality: A review. *Geol. Ecol. Landsc.* **2017**, *1*, 1–11. [CrossRef]
3. Eswaran, H.; Lal, R.; Reich, P.F. Land Degradation: An Overview. In *Responses to Land Degradation*; Bridges, E.M., Hannam, I.D., Oldeman, L.R., de Vries, P.F.W.T., Scher, S.J., Sompatpanit, S., Eds.; CRC Press: Boca Raton, FL, USA, 2001; pp. 20–35. [CrossRef]
4. Tun, K.K.; Shrestha, R.P.; Datta, A. Assessment of land degradation and its impact on crop production in the Dry Zone of Myanmar. *Int. J. Sustain. Dev. World Ecol.* **2015**, *22*, 533–544. [CrossRef]
5. Zhang, X.; Wenhong, C.; Qingchao, G.; Sihong, W. Effects of landuse change on surface runoff and sediment yield at different watershed scales on the Loess Plateau. *Int. J. Sediment Res.* **2010**, *25*, 283–293. [CrossRef]
6. Aswathi, J.; Sajinkumar, K.; Rajaneesh, A.; Oommen, T.; Bouali, E.; Binojkumar, R.; Rani, V.; Thomas, J.; Thrivikramji, K.; Ajin, R.; et al. Furthering the precision of RUSLE soil erosion with PSInSAR data: An innovative model. *Geocarto Int.* **2022**, *37*, 16108–16131. [CrossRef]
7. Wijitkosum, S. Factor influencing land degradation sensitivity and desertification in a drought prone watershed in Thailand. *Int. Soil Water Conserv. Res.* **2021**, *9*, 217–228. [CrossRef]
8. Duda, A.M. Environmental and economic damage caused by sediment from agricultural nonpoint sources. *J. Am. Water Resour. Assoc.* **1985**, *21*, 225–234. [CrossRef]
9. Wang, G.; Gertner, G.; Fang, S.; Anderson, A.B. Mapping multiple variables for predicting soil loss by geostatistical methods with TM images and a slope map. *Photogramm. Eng. Remote Sens.* **2003**, *8*, 889–898. [CrossRef]
10. Liu, X.; Li, H.; Zhang, S.; Cruse, R.M.; Zhang, X. Gully Erosion Control Practices in Northeast China: A Review. *Sustainability* **2019**, *11*, 5065. [CrossRef]
11. Morera, S.B.; Condom, T.; Vauchel, P.; Guyot, J.L.; Galvez, C.; Crave, A. Pertinent spatio-temporal scale of observation to understand suspended sediment yield control factors in the Andean region: The case of the Santa River (Peru). *Hydrol. Earth Syst. Sci.* **2013**, *17*, 4641–4657. [CrossRef]
12. Marondedze, A.K.; Schütt, B. Assessment of Soil Erosion Using the RUSLE Model for the Epworth District of the Harare Metropolitan Province, Zimbabwe. *Sustainability* **2020**, *12*, 8531. [CrossRef]
13. Martınez-Casasnovas, J.A.; Ramos, M.C.; Ribes-Dasi, M. Soil erosion caused by extreme rainfall events: Mapping and quantification in agricultural plots from very detailed digital elevation models. *Geoderma* **2002**, *105*, 125–140. [CrossRef]
14. Merritt, W.S.; Letcher, R.A.; Jakeman, A.J. A review of erosion and sediment transport models. *Environ. Model. Softw.* **2003**, *18*, 761–799. [CrossRef]
15. De Vente, J.; Poesen, J. Predicting soil erosion and sediment yield at the basin scale: Scale issues and semi-quantitative models. *Earth Sci. Rev.* **2005**, *71*, 95–125. [CrossRef]
16. Fu, G.; Chen, S.; McCool, D.K. Modeling the impacts of no-till practice on soil erosion and sediment yield with RUSLE, SEDD, and ArcView GIS. *Soil. Tillage Res.* **2006**, *85*, 38–49. [CrossRef]
17. Boardman, J.; Poesen, J. *Soil Erosion in Europe*; Wiley: New York, NY, USA, 2006. [CrossRef]
18. Wischmeier, W.H.; Smith, D.D. *Predicting Rainfall Erosion Losses: A Guide to Conservation Planning*; US Department of Agriculture, Science and Education Administration: Washington, DC, USA, 1978.
19. Renard, K.; Foster, G.; Weesies, G.; McCool, D.; Yoder, D. *Predicting Soil Erosion by Water: A Guide to Conservation Planning with the Revised Universal Soil Loss Equation (RUSLE)*; United States Government Printing: Washington, DC, USA, 1997; p. 404.
20. Sundara Kumar, P.; Praveen, T.V.; Prasad, A. Simulation of sediment yield over un-gauged stations using MUSLE and Fuzzy Model. *Aquat. Procedia* **2015**, *4*, 1291–1298. [CrossRef]
21. Grum, B.; Woldearegay, K.; Hessel, R.; Baartman, J.E.M.; Abdulkadir, M.; Yazew, E.; Kessler, A.; Ritsema, C.J.; Geissen, V. Assessing the Effect of Water Harvesting Techniques on Event-Based Hydrological Responses and Sediment Yield at a Catchment Scale in Northern Ethiopia Using the Limburg Soil Erosion Model (LISEM). *Catena* **2017**, *159*, 20–34. [CrossRef]
22. Morgan, R.P.C.; Morgan, D.D.V.; Finney, H.J. A predictive model for the assessment of soil erosion risk. *J. Agric. Eng. Res.* **1984**, *30*, 245–253. [CrossRef]
23. Shrestha, D.P.; Jetten, V.G. Modelling erosion on a daily basis, an adaptation of the MMF approach. *Int. J. Appl. Earth Obs. Geoinf.* **2018**, *64*, 117–131. [CrossRef]
24. Quijano, L.; Beguería, S.; Gaspar, L.; Navas, A. Estimating erosion rates using 137Cs measurements and WATEM/SEDEM in a Mediterranean cultivated field. *Catena* **2016**, *138*, 38–51. [CrossRef]
25. Vigiak, O.; Malagó, A.; Bouraoui, F.; Vanmaercke, M.; Poesen, J. Adapting SWAT hillslope erosion model to predict sediment concentration sand yields in large Basins. *Sci. Total Environ.* **2015**, *538*, 855–875. [CrossRef] [PubMed]
26. Pieri, L.; Bittelli, M.; Wu, J.Q.; Dun, S.; Flanagan, D.C.; Rossi Pisa, P.; Ventura, F.; Salvatorelli, F. Using the Water Erosion Prediction Project (WEPP) model to simulate field observed runoff and erosion in the Apennines Mountain range, Italy. *J. Hydrol.* **2007**, *336*, 84–97. [CrossRef]
27. Morgan, R.P.C.; Quinton, J.N.; Smith, R.E.; Govers, G.; Poesen, J.W.A.; Auerswald, K.; Chisci, G.; Torri, D.; Styczen, M.E. The European Soil Erosion Model (EUROSEM): A dynamic approach for predicting sediment transport from fields and small catchments. *Earth Surf. Process. Landf.* **1998**, *23*, 527–544. [CrossRef]

28. Gavrilovic, S. A method for estimating the average annual quantity of sediments according to the potency of erosion. *Bull. Fac. For.* **1962**, *26*, 151–168.
29. Gavrilovic, S. Modern ways of calculating the torrential sediment and erosion mapping. In *Erosion, Torrents and Alluvial Deposits*; Yugoslav Committee for International Hydrological Decade: Belgrade, Serbia, 1970; pp. 85–100.
30. Tošić, R.; Dragićević, S.; Lovrić, N. Assessment of soil erosion and sediment yield changes using erosion potential model–case study: Republic of Srpska (BiH). *Carpathian J. Earth Environ. Sci.* **2012**, *7*, 147–154.
31. Gavrilovic, Z. Use of an empirical method (Erosion Potential Method) for calculating sediment production and transportation in unstudied or torrential streams. In *International Conference on River Regime*; Hydraulics Research Ltd.: Wallingford, UK, 1988; pp. 411–422.
32. Kostadinov, S.; Braunović, S.; Dragićević, S.; Zlatić, M.; Dragović, N.; Rakonjac, N. Effects of Erosion Control Works: Case Study—Grdelica Gorge, the South Morava River (Serbia). *Water* **2018**, *10*, 1094. [CrossRef]
33. Echogdali, F.Z.; Boutaleb, S.; Kpan, R.B.; Ouchchen, M.; Bendarma, A.; El Ayady, H.; Abdelrahman, K.; Fnais, M.S.; Sajinkumar, K.S.; Abioui, M. Application of Fuzzy Logic and Fractal Modeling Approach for Groundwater Potential Mapping in Semi-Arid Akka Basin, Southeast Morocco. *Sustainability* **2022**, *14*, 10205. [CrossRef]
34. Xie, F.; Zhao, G.; Mu, X.; Tian, P.; Gao, P.; Sun, W. Sediment Yield in Dam-Controlled Watersheds in the Pisha Sandstone Region on the Northern Loess Plateau, China. *Land* **2021**, *10*, 1264. [CrossRef]
35. Fanetti, D.; Vezzoli, L. Sediment input and evolution of lacustrine deltas: The Breggia and Greggio rivers case study (Lake Como, Italy). *Quat. Int.* **2007**, *173*, 113–124. [CrossRef]
36. De Vente, J.; Poesen, J.; Bazzoffi, P.; Rompaey, A.V.; Verstraeten, G. Predicting catchment sediment yield in Mediterranean environments: The importance of sediment sources and connectivity in Italian drainage basins. *Earth Surf. Process. Landf.* **2006**, *31*, 1017–1034. [CrossRef]
37. Koirala, P.; Thakuri, S.; Joshi, S.; Chauhan, R. Estimation of Soil Erosion in Nepal Using a RUSLE Modeling and Geospatial Tool. *Geosciences* **2019**, *9*, 147. [CrossRef]
38. Gocić, M.; Dragićević, S.; Radivojević, A.; Martić Bursać, N.; Stričević, L.; Đorđević, M. Changes in Soil Erosion Intensity Caused by Land Use and Demographic Changes in the Jablanica River Basin, Serbia. *Agriculture* **2020**, *10*, 345. [CrossRef]
39. Emmanouloudis, D.A.; Christou, O.P.; Filippidis, E. Quantitative estimation of degradation in the Alikamon river basin using GIS. In *Erosion Prediction in Ungauged Basins: Integrating Methods and Techniques*; De Boer, D., Froehlich, W., Mizuyama, T., Pietroniro, A., Eds.; IAHS Publication: Wallingford, UK, 2003; Volume 279.
40. Sinha, A.; Nikhil, S.; Ajin, R.S.; Danumah, J.H.; Saha, S.; Costache, R.; Rajaneesh, A.; Sajinkumar, K.S.; Amrutha, K.; Johny, A.; et al. Wildfire Risk Zone Mapping in Contrasting Climatic Conditions: An Approach Employing AHP and F-AHP Models. *Fire* **2023**, *6*, 44. [CrossRef]
41. Margiorou, S.; Kastridis, A.; Sapountzis, M. Pre/Post-Fire Soil Erosion and Evaluation of Check-Dams Effectiveness in Mediterranean Suburban Catchments Based on Field Measurements and Modeling. *Land* **2022**, *11*, 1705. [CrossRef]
42. Kastridis, A.; Stathis, D.; Sapountzis, M.; Theodosiou, G. Insect Outbreak and Long-Term Post-Fire Effects on Soil Erosion in Mediterranean Suburban Forest. *Land* **2022**, *11*, 911. [CrossRef]
43. Depountis, N.; Michalopoulou, M.; Kavoura, K.; Nikolakopoulos, K.; Sabatakakis, N. Estimating Soil Erosion Rate Changes in Areas Affected by Wildfires. *ISPRS Int. J. Geo-Inf.* **2020**, *9*, 562. [CrossRef]
44. Benchettouh, A.; Kouri, L.; Jebari, S. Spatial estimation of soil erosion risk using RUSLE/GIS techniques and practices conservation suggested for reducing soil erosion in Wadi Mina watershed (northwest, Algeria). *Arab. J. Geosci.* **2017**, *10*, 79. [CrossRef]
45. Kastridis, A.; Margiorou, S.; Sapountzis, M. Check-Dams and Silt Fences: Cost-Effective Methods to Monitor Soil Erosion under Various Disturbances in Forest Ecosystems. *Land* **2022**, *11*, 2129. [CrossRef]
46. Bensekhria, A.; Bouhata, R. Assessment and Mapping Soil Water Erosion Using RUSLE Approach and GIS Tools: Case of Oued el-Hai Watershed, Aurès West, Northeastern of Algeria. *ISPRS Int. J. Geo-Inf.* **2022**, *11*, 84. [CrossRef]
47. Hategekimana, Y.; Allam, M.; Meng, Q.; Nie, Y.; Mohamed, E. Quantification of Soil Losses along the Coastal Protected Areas in Kenya. *Land* **2020**, *9*, 137. [CrossRef]
48. Covelli, C.; Cimorelli, L.; Pagliuca, D.N.; Molino, B.; Pianese, D. Assessment of Erosion in River Basins: A Distributed Model to Estimate the Sediment Production over Watersheds by a 3-Dimensional LS Factor in RUSLE Model. *Hydrology* **2020**, *7*, 13. [CrossRef]
49. Tahouri, J.; Sadiki, A.; Karrat, L.; Johnson, V.C.; Weng Chan, N.; Fei, Z.; Te Kung, H. Using a modified PAP/RAC model and GIS-for mapping water erosion and causal risk factors: Case study of the Asfalou watershed, Morocco. *Int. Soil. Water Conserv. Res.* **2022**, *10*, 254–272. [CrossRef]
50. Pham, T.G.; Degener, J.; Kappas, M. Integrated universal soil loss equation (USLE) and Geographical Information System (GIS) for soil erosion estimation in A Sap basin: Central Vietnam. *Int. Soil. Water Conserv. Res.* **2018**, *6*, 99–110. [CrossRef]
51. Fistikoglu, O.; Harmancioglu, N.B. Integration of GIS with USLE in assessment of soil erosion. *Water Resour. Manag.* **2002**, *16*, 447–467. [CrossRef]
52. Parveen, R.; Kumar, U. Integrated approach of universal soil loss equation (USLE) and geographical information system (GIS) for soil loss risk assessment in Upper South Koel Basin, Jharkhand. *J. Geogr. Inf. Syst.* **2012**, *4*, 588–596. [CrossRef]
53. Dominici, R.; Larosa, S.; Viscomi, A.; Mao, L.; De Rosa, R.; Cianflone, G. Yield Erosion Sediment (YES): A PyQGIS Plug-In for the Sediments Production Calculation Based on the Erosion Potential Method. *Geosciences* **2020**, *10*, 324. [CrossRef]

54. Mohammadi, M.; Khaledi Darvishan, A.K.; Spalevic, V.; Dudic, B.; Billi, P. Analysis of the Impact of Land Use Changes on Soil Erosion Intensity and Sediment Yield Using the IntErO Model in the Talar Watershed of Iran. *Water* **2021**, *13*, 881. [CrossRef]
55. Ali, S.A.; Hagos, H. Estimation of soil erosion using USLE and GIS in Awassa Catchment, Rift valley, Central Ethiopia. *Geoderma Reg.* **2016**, *7*, 159–166. [CrossRef]
56. Echogdali, F.Z.; Boutaleb, S.; Taia, S.; Ouchchen, M.; Id–Belqas, M.; Kpan, R.B.; Abioui, M.; Aswathi, J.; Sajinkumar, K.S. Assessment of soil erosion risk in a semi–arid climate watershed using SWAT model: Case of Tata basin, South–East of Morocco. *Appl. Water Sci.* **2022**, *12*, 137. [CrossRef]
57. Elaloui, A.; Khalki, E.M.E.; Namous, M.; Ziadi, K.; Eloudi, H.; Faouzi, E.; Bou-Imajjane, L.; Karroum, M.; Tramblay, Y.; Boudhar, A.; et al. Soil Erosion under Future Climate Change Scenarios in a Semi-Arid Region. *Water* **2023**, *15*, 146. [CrossRef]
58. Diani, K.; Ettazarini, S.; Hahou, Y.; El Belrhiti, H.; Allaoui, W.; Mounir, K.; Gourfi, A. Identification of soil erosion sites in semiarid zones: Using GIS, remote sensing, and PAP/RAC model. In *Handbook of Hydroinformatics*; Eslamian, S., Eslamian, F., Eds.; Elsevier: Amsterdam, The Netherlands, 2023; pp. 169–183. [CrossRef]
59. Aït Hssaine, A. Éléments sur l'hydrologie de la partie atlasique de l'oued Guir (Maroc sud-oriental) et sur l'inondation catastrophique du 10 octobre 2008. *Physio-Géo* **2014**, *8*, 337–354. [CrossRef]
60. Kogo, B.K.; Kumar, L.; Koech, R. Impact of Land Use/Cover Changes on Soil Erosion in Western Kenya. *Sustainability* **2020**, *12*, 9740. [CrossRef]
61. Hembram, T.K.; Paul, G.C.; Saha, S. Comparative analysis between morphometry and geo-environmental factor based soil erosion risk assessment using weight of evidence model: A study on Jainti river basin, eastern India. *Environ. Process.* **2019**, *6*, 883–913. [CrossRef]
62. Chaaouan, J.; Faleh, A.; Sadiki, A.; Mesrar, H. Télédétection, SIG et modélisation de l'érosion hydrique dans le bassin versant de l'oued Amzaz, Rif Central. *Rev. Fr. Photogramm. Télédetect.* **2013**, *203*, 19–25. [CrossRef]
63. Ewunetu, A.; Simane, B.; Teferi, E.; Zaitchik, B.F. Mapping and Quantifying Comprehensive Land Degradation Status Using Spatial Multicriteria Evaluation Technique in the Headwaters Area of Upper Blue Nile River. *Sustainability* **2021**, *13*, 2244. [CrossRef]
64. Spalevic, V.; Barovic, G.; Vujacic, D.; Curovic, M.; Behzadfar, M.; Djurovic, N.; Dudic, B.; Billi, P. The Impact of Land Use Changes on Soil Erosion in the River Basin of Miocki Potok, Montenegro. *Water* **2020**, *12*, 2973. [CrossRef]
65. Zingg, A.W. Degree and length of land slope as it affects soil loss in run-off. *Agric. Eng.* **1940**, *21*, 59–64.
66. Mohammed, S.; Al-Ebraheem, A.; Holb, I.J.; Alsafadi, K.; Dikkeh, M.; Pham, Q.B.; Linh, N.T.T.; Szabo, S. Soil Management Effects on Soil Water Erosion and Runoff in Central Syria—A Comparative Evaluation of General Linear Model and Random Forest Regression. *Water* **2020**, *12*, 2529. [CrossRef]
67. Echogdali, F.Z.; Boutaleb, S.; Bendarma, A.; Saidi, M.E.; Aadraoui, M.; Abioui, M.; Ouchchen, M.; Abdelrahman, K.; Fnais, M.S.; Sajinkumar, K.S. Application of Analytical Hierarchy Process and Geophysical Method for Groundwater Potential Mapping in the Tata Basin, Morocco. *Water* **2022**, *14*, 2393. [CrossRef]
68. Mohammed, S.; Abdo, H.G.; Szabo, S.; Pham, Q.B.; Holb, I.J.; Linh, N.T.T.; Tram Anh, D.; Alsafadi, K.; Mokhtar, A.; Kbibo, I.; et al. Estimating human impacts on soil erosion considering different hillslope inclinations and land uses in the coastal region of Syria. *Water* **2020**, *12*, 2786. [CrossRef]
69. Römkens, M.J.; Helming, K.; Prasad, S.N. Soil erosion under different rainfall intensities, surface roughness, and soil water regimes. *Catena* **2002**, *46*, 103–123. [CrossRef]
70. Alexakis, D.D.; Hadjimitsis, D.G.; Agapiou, A. Integrated use of remote sensing, GIS and precipitation data for the assessment of soil erosion rate in the catchment area of "Yialias" in Cyprus. *Atmos. Res.* **2013**, *131*, 108–124. [CrossRef]
71. Cerdan, O. Analyse et Modélisation du Transfert de Particules Solides à l'échelle de Petits Bassins Versants Cultives. Ph.D. Thesis, Université d'Orléans, Orléans, France, 2001.
72. Cerdan, O.; Delmas, M.; Négrel, P.; Mouchel, J.M.; Petelet-Giraud, E.; Salvador-Blanes, S.; Degan, F. Contribution of diffuse hillslope erosion to the sediment export of French rivers. *C. R. Geosci.* **2012**, *344*, 636–645. [CrossRef]
73. Rey, F.; Ballais, J.L.; Marre, A.; Rovéra, G. Rôle de la végétation dans la protection contre l'érosion hydrique de surface. *C. R. Geosci.* **2004**, *336*, 991–998. [CrossRef]
74. Xian, G.; Shi, H.; Dewitz, J.; Wu, Z. Performances of WorldView 3, Sentinel 2, and Landsat 8 data in mapping impervious surface. *Remote Sens. Appl. Soc. Environ.* **2019**, *15*, 100246. [CrossRef]
75. Sánchez-Espinosa, A.; Schröder, C. Land use and land cover mapping in wetlands one step closer to the ground: Sentinel-2 versus Landsat 8. *J. Environ. Manag.* **2019**, *247*, 484–498. [CrossRef]
76. Pflugmacher, D.; Rabe, A.; Peters, M.; Hostert, P. Mapping pan-European land cover using Landsat spectral-temporal metrics and the European LUCAS survey. *Remote Sens. Environ.* **2019**, *221*, 583–595. [CrossRef]
77. Chikh, H.A.; Habi, M.; Morsli, B. Influence of vegetation cover on the assessment of erosion and erosive potential in the Isser marly watershed in northwestern Algeria—Comparative study of RUSLE and PAP/RAC methods. *Arab. J. Geosci.* **2019**, *12*, 154. [CrossRef]
78. Kostyuchenko, Y.; Artemenko, I.; Abioui, M.; Benssaou, M. Global and Regional Climatic Modeling. In *Encyclopedia of Mathematical Geosciences*; Sagar, B.D., Cheng, Q., McKinley, J., Agterberg, F., Eds.; Springer: Cham, Switzerland, 2022; pp. 1–5. [CrossRef]
79. Simonneaux, V.; Cheggour, A.; Deschamps, C.; Mouillot, F.; Cerdan, O.; Le Bissonnais, Y. Land use and climate change effects on soil erosion in a semi-arid mountainous watershed (High Atlas, Morocco). *J. Arid. Environ.* **2015**, *122*, 64–75. [CrossRef]

80. Aslam, B.; Maqsoom, A.; Alaloul, W.S.; Musarat, M.A.; Jabbar, T.; Zafar, A. Soil erosion susceptibility mapping using a GIS-based multi-criteria decision approach: Case of district Chitral, Pakistan. *Ain Shams Eng. J.* **2021**, *12*, 1637–1649. [CrossRef]
81. Molina, A.; Govers, G.; Vanacker, V.; Poesen, J.; Zeelmaekers, E.; Cisneros, F. Runoff generation in a degraded Andean ecosystem: Interaction of vegetation cover and land use. *Catena* **2007**, *71*, 357–370. [CrossRef]
82. Nunes, A.N.; de Almeida, A.C.; Coelho, C.O.A. Impact of land use and cover type on runoff and erosion in a marginal area of Portugal. *Appl. Geogr.* **2011**, *31*, 687–699. [CrossRef]
83. Wei, W.; Chen, L.D.; Fu, B.J. Effects of rainfall change on water erosion processes in terrestrial ecosystems: A review. *Prog. Phys. Geogr.* **2009**, *33*, 307–318. [CrossRef]
84. Wei, W.; Chen, L.D.; Fu, B.J.; Lü, Y.H.; Gong, J. Responses of water erosion to rainfall extremes and vegetation types in a loess semiarid hilly area, NW China. *Hydrol. Process.* **2009**, *23*, 1780–1791. [CrossRef]
85. Kim, K.; Jeong, Y. Hydrological variations of discharge, soil loss and recession coefficient in three small forested catchments. In *Environmental Forest Science*; Sassa, K., Ed.; Springer: Dordrecht, The Netherlands, 1998; pp. 431–438. [CrossRef]
86. Elbadaoui, K.; Algouti, A.; Algouti, A.; Aitmlouk, M.; Abdelouhed, F. Flood risk modelling using hydrologic data, HECRAS and GIS tools: Case of Toudgha River (Tinghir, Morocco). *Disaster Adv.* **2020**, *13*, 1–13.
87. Benjmel, K.; Amraoui, F.; Aydda, A.; Tahiri, A.; Yousif, M.; Pradhan, B.; Abdelrahman, K.; Fnais, M.S.; Abioui, M. A multidisciplinary approach for groundwater potential mapping in a fractured semi-arid terrain (Kerdous Inlier, Western Anti-Atlas, Morocco). *Water* **2022**, *14*, 1553. [CrossRef]
88. Abioui, M.; Ikirri, M.; Boutaleb, S.; Faik, F.; Wanaim, A.; Id-Belqas, M.; Echogdali, F.Z. GIS for Watershed Characterization and Modeling: Example of the Taguenit River (Lakhssas, Morocco). In *Water, Land, and Forest Susceptibility and Sustainability: Geospatial Approaches and Modeling*; Chatterjee, U., Pradhan, B., Kumar, S., Saha, S., Zakwan, M., Eds.; Elsevier: Amsterdam, The Netherlands, 2023; pp. 61–85. [CrossRef]